

Virtual Holonomic Constraint Based Direction Following Control of Planar Snake Robots Described by a Simplified Model

Ehsan Rezapour, Andreas Hofmann, Kristin Y. Pettersen, Alireza Mohammadi, and Manfredi Maggiore

Abstract—This paper considers direction following control of planar snake robots for which the equations of motion are described based on a simplified model. In particular, we aim to regulate the orientation and the forward velocity of the robot to a constant vector, while guaranteeing the boundedness of the states of the controlled system. To this end, we first stabilize a constraint manifold for the fully-actuated body shape variables of the robot. The definition of the constraint manifold is inspired by the well-known reference joint angle trajectories which induce lateral undulatory motion for snake robots. Subsequently, we reduce the dynamics of the system to the invariant constraint manifold. Furthermore, we design two dynamic compensators which control the orientation and velocity of the robot on this manifold. Using numerical analysis and a formal stability proof, we show that the solutions of the dynamic compensators remain bounded. Numerical simulations are presented to validate the theoretical design.

I. INTRODUCTION

Snake robots are a class of vehicle-manipulator robots which are inspired by the structural characteristics of biological snakes. In particular, these robots are characterized by a hyper-redundant structure which enables them to robustly traverse challenging terrains. Furthermore, their narrow body enables them to effectively perform in narrow and unstructured environments. This has made them an interesting alternative for many emerging medical [1], industrial [2], and search and rescue operations [3].

Locomotion control of snake robots has been considered in several previous works. For wheeled snake robots, which are subject to nonholonomic velocity constraints, the control input is usually specified directly in terms of the desired propulsion of the snake robot. This method is employed in e.g. [4-8] for computed torque control of the position and orientation of wheeled snake robots.

Locomotion control of wheel-less snake robots is only considered in a few previous works. Locomotion Mecha-

nism in wheel-less snake robots is more similar to their biological counterparts. These robots are more interesting for traversing even more challenging environments where the passive wheels may slip or get tangled up in irregularities in the terrain. Methods based on numerical optimal control are considered in [9] for determining optimal gaits during positional control of wheel-less snake robots. In [10,11], cascaded systems theory is employed to achieve path following control of a wheel-less snake robot described by a simplified model. In [12], a dynamic feedback control law is used to control the orientation of the robot to a reference angle defined by a path following guidance law.

This paper considers direction following control of planar snake robots. In direction following control, the goal is to regulate the velocity of the center of mass (CM) of the robot to a constant reference, while guaranteeing the boundedness of the system states. The primary idea of the control design is presented in [20], and here we adapt the results to a different model of the snake robots which is presented in [10], and is more amenable to model-based control design.

In general, application of the analytically designed automatic control approaches which rely on formal stability proofs for snake robots is challenging. This is due to the complex dynamical behaviour of these hyper-redundant robots. Furthermore, snake robots are a class of underactuated robots, which are characterized by lack of direct independent control input for (at least) three degrees of freedom of the system. Moreover, it is known that the control of underactuated mechanical systems is a challenging and open area of research. Snake robots, which pose challenging underactuated control problems, can thus be considered as a valuable benchmark example for theoretical developments on underactuated mechanical systems.

In the current work, we use the method of virtual holonomic constraints (VHC) to solve the direction following control problem for a wheel-less snake robot. The idea of VHC has previously been used as an effective tool for motion control of mechanical systems, see e.g. [14-16]. It was used for snake robot locomotion in [12] to control the orientation of a wheel-less snake robot, but the velocity of the snake robot was not controlled. Using the VHC approach, we confine the state evolution of a mechanical system to an invariant constraint manifold. In case of the snake robot, we perform this by enforcing appropriately defined VHC which induce a lateral undulatory locomotion on the robot. Furthermore, we then will show that the dynamical system reduced to the invariant constraint manifold can effectively be controlled using two dynamic compensators. In particular, we will use a dynamic compensator which adds an offset angle to each link in order to reorient the robot in the plane,

E. Rezapour and K. Y. Pettersen were partly supported by the Research Council of Norway through the Centres of Excellence funding scheme, project No. 223254 AMOS, and project No. 205622. A. Mohammadi and M. Maggiore were supported by the Natural Sciences and Engineering Research Council (NSERC) of Canada.

E. Rezapour, and K. Y. Pettersen are with the Department of Engineering Cybernetics, Norwegian University of Science and Technology, NO-7491 Trondheim, Norway. emails: {ehsan.rezapour, kristin.y.pettersen}@itk.ntnu.no

The affiliation of A. Hofmann is shared between the Department of Engineering Cybernetics, Norwegian University of Science and Technology, and the Institute for Systems, Theory and Automatic Control, University of Stuttgart. email: andreas.hofmann@stud.uni-stuttgart.de

A. Mohammadi and M. Maggiore are with the Department of Electrical and Computer Engineering, University of Toronto, 10 Kings College Road, Toronto, ON M5S 3G4, Canada. emails: {alireza.mohammadi@mail.utoronto.ca, maggiore@control.utoronto.ca}

in accordance with a reference orientation angle. Moreover, using another dynamic compensator we will employ the frequency of the periodic body oscillations given by the gait pattern lateral undulation, to regulate the forward velocity of the robot to a constant vector. Using numerical simulations and formal stability proofs, we show that the solutions of these dynamic compensators remain bounded, respectively. Showing the boundedness of the solutions of the dynamic compensator which controls the orientation by using numerical simulations, i.e. along particular solutions, is a theoretical gap which will remain as a topic of future works.

The paper is organized as follows. In Section II, we present simplified kinematic and dynamic models of a planar snake robot. In Section III, the control design objectives are stated. In Section IV, we propose a dynamic feedback control law to control the body shape of the robot. In Section V, we design an orientation controller for the robot. In Section VI, a velocity controller is proposed. In Section VII, simulation results are presented to validate the theoretical approach.

II. MODELLING

In this section, for completeness of the paper, we briefly present a simplified model of the snake robot dynamics that can effectively be used for the model-based control design in the subsequent sections. This model was designed for control design and analysis purposes, and is thoroughly presented in [10], where it is validated both through numerical simulations and real time experiments. Furthermore, in [10] it is shown that the fundamental properties of the simplified model such as stabilizability and controllability, are essentially the same as the more complex models presented in several previous works, see e.g. [4,5,12].

A. Notation

In this subsection, we introduce the following notations, which will be used throughout the paper to simplify the equations.

$$0_{N-1} = [0, \dots, 0]^T \in \mathbb{R}^{N-1} \quad (1)$$

$$\bar{e} = [1, \dots, 1]^T \in \mathbb{R}^{N-1} \quad (2)$$

$$A = \begin{bmatrix} 1 & 1 & & & \\ & \ddots & \ddots & & \\ & & \ddots & \ddots & \\ & & & 1 & 1 \end{bmatrix} \in \mathbb{R}^{(N-1) \times N} \quad (3)$$

$$D = \begin{bmatrix} 1 & -1 & & & \\ & \ddots & \ddots & & \\ & & \ddots & \ddots & \\ & & & 1 & -1 \end{bmatrix} \in \mathbb{R}^{(N-1) \times N} \quad (4)$$

$$\bar{D} = D^T(DD^T)^{-1} \in \mathbb{R}^{N \times (N-1)} \quad (5)$$

Furthermore, N denotes the number of links, l denotes the length of the links, and m denotes the uniformly distributed mass of the links, respectively.

B. A simplified model of the snake robot

Kinematic and dynamic models of snake robots are previously derived in several works (see e.g., [4,5,10,12]).

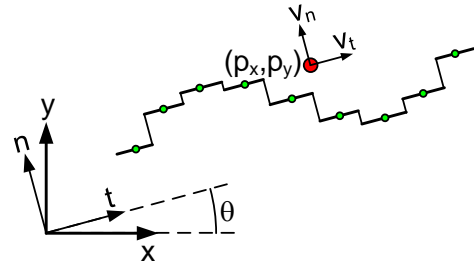


Fig. 1: Illustration of two coordinate frames used in the simplified model. The $x - y$ frame is fixed, and the $t - n$ frame is always aligned with the snake robot.

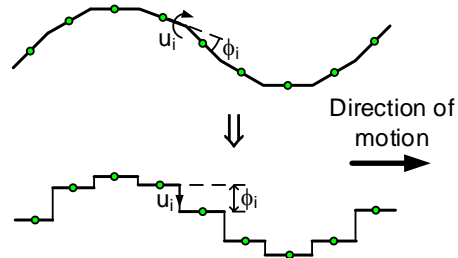


Fig. 2: The snake robot is modelled using a series of prismatic joints which move the robot forward by translational displacements. u_i is the exerted torque or force in the i -th joint of the robot.

All these models share the same property that they are very complex for analytical investigations. The derivation of the simplified model of snake robot dynamics in [10] is motivated by the attractive idea that these complex dynamic models contain nonlinear dynamics that are not essential to the overall locomotion of the robot. Moreover, proper approximations of these nonlinear dynamics with simpler mathematical descriptions can significantly simplify the analysis and model-based control design for snake robots.

C. An overview of the simplified modelling approach

In this subsection, we review the simplified modelling approach presented in [10]. It is known [10] that lateral undulation mainly consists of link displacements which are transversal to the direction of motion. Moreover, this transversal link displacements induce the forward motion on snake robots. The main idea behind the simplified model of the snake robot dynamics is to map the periodic body shape changes to forward propulsion, through mapping the rotational joint motion to translational link displacements, cf. Fig. 2. Since the translational displacements are in general less complex than rotational motion, this will simplify the resulting dynamic model of the robot.

D. Simplified kinematic and dynamic equations

In this subsection, we present the simplified kinematic and dynamic models of a wheel-less snake robot which moves on a horizontal and flat surface. Based on the illustrations of the robot in Fig. 1-2, we choose the elements of the vector of the generalized coordinates, which represent the configuration space \mathcal{Q} of the robot, as

$$x = [\phi_1, \dots, \phi_{N-1}, \theta, p_x, p_y]^T \in \mathbb{R}^{N+2} \quad (6)$$

where ϕ_i denotes the i -th joint angle, θ denotes the orientation, and (p_x, p_y) denotes the planar position of the CM of the robot. We denote the vector of the joint angles of the robot by $\phi = [\phi_1, \dots, \phi_{N-1}]^T \in \mathbb{R}^{N-1}$. The elements of ϕ are called the body shape variables, which define the internal configuration of the robot. The vector of the generalized velocities is defined as the time-derivative of (6) as

$$\dot{x} = [v_{\phi_1}, \dots, v_{\phi_{N-1}}, v_\theta, \dot{p}_x, \dot{p}_y]^T \in \mathbb{R}^{N+2} \quad (7)$$

We denote the vector of the joint velocities by $v_\phi = [v_{\phi_1}, \dots, v_{\phi_{N-1}}]^T \in \mathbb{R}^{N-1}$. Since we aim to control the forward and normal velocities of the robot, we map the inertial velocity of the CM of the robot to the $t-n$ frame which is always aligned with the robot, cf. Fig. 1, as

$$\dot{p}_x = v_t \cos(\theta) - v_n \sin(\theta) \quad (8)$$

$$\dot{p}_y = v_t \sin(\theta) + v_n \cos(\theta) \quad (9)$$

where $v_t \in \mathbb{R}$ and $v_n \in \mathbb{R}$ denote the tangential and normal components of the inertial velocity of the CM mapped into the direction of motion of the robot, respectively. The simplified dynamic model of the robot w.r.t. (x, \dot{x}) can be represented as [10]

$$\dot{\phi} = v_\phi \quad (10)$$

$$\dot{\theta} = v_\theta \quad (11)$$

$$\dot{p}_x = v_t \cos(\theta) - v_n \sin(\theta) \quad (12)$$

$$\dot{p}_y = v_t \sin(\theta) + v_n \cos(\theta) \quad (13)$$

$$\dot{v}_\phi = -\frac{c_n}{m} v_\phi + \frac{c_p}{m} v_t A D^T \phi + \frac{1}{m} D D^T u \quad (14)$$

$$\dot{v}_\theta = -\lambda_1 v_\theta + \frac{\lambda_2}{N-1} v_t \bar{e}^T \phi \quad (15)$$

$$\dot{v}_t = -\frac{c_t}{m} v_t + \frac{2c_p}{Nm} v_n \bar{e}^T \phi - \frac{c_p}{Nm} \phi^T A \bar{D} v_\phi \quad (16)$$

$$\dot{v}_n = -\frac{c_n}{m} v_n + \frac{2c_p}{Nm} v_t \bar{e}^T \phi \quad (17)$$

where $c_n \in \mathbb{R}_{>0}$ and $c_t \in \mathbb{R}_{>0}$ denote the viscous friction coefficients in the normal and tangential direction of motion of the links, respectively. Moreover, $\lambda_1 \in \mathbb{R}_{>0}$, $\lambda_2 \in \mathbb{R}_{>0}$ are used to describe the mapping from the rotational motion to the prismatic motion (see [10]). Furthermore, c_p is defined as $c_p = \frac{c_n - c_t}{2l} \in \mathbb{R}_{>0}$.

Using feedback linearization of the dynamics of the fully-actuated degrees of freedom of the robot, i.e. the joint angles ϕ , we perform the following change of the vector of the control inputs:

$$u = m(DD^T)^{-1} \left(\bar{u} + \frac{c_n}{m} v_\phi - \frac{c_p}{m} v_t A D^T \phi \right) \quad (18)$$

where $\bar{u} = [\bar{u}_1, \dots, \bar{u}_{N-1}]^T \in \mathbb{R}^{N-1}$ is the new set of control inputs. Inserting (18) into (14), transforms the dynamics of the joint angles into

$$\dot{v}_\phi = \bar{u} \quad (19)$$

The simplified dynamic model (10-17) is suitable for the model-based direction following control design which will be presented in the following sections.

III. CONTROL DESIGN OBJECTIVES

In this section, we present the control design objectives for the controllers in the subsequent sections. In direction following control, the objective is to regulate the linear velocity vector of the snake robot to a constant reference, while guaranteeing the boundedness of the system states. According to this definition, we define the following control objectives for the snake robot.

The first control objective concerns the body shape of the robot. Given the desired periodic body motions, i.e., a desired gait pattern, which we denote by $\phi_{\text{ref}}(t) \in \mathbb{R}^{N-1}$, we aim to asymptotically stabilize the desired gait pattern for the body shape variables of the robot such that

$$\lim_{t \rightarrow \infty} \|\phi(t) - \phi_{\text{ref}}(t)\| = 0 \quad (20)$$

Furthermore, we seek to control the orientation of the robot. Thus, the second control objective is to stabilize a constant reference orientation θ_{ref} for the robot such that

$$\lim_{t \rightarrow \infty} \|\theta(t) - \theta_{\text{ref}}\| = 0 \quad (21)$$

The third control objective concerns the velocity of the robot. In particular, we aim to practically stabilize (see e.g. [17]) a constant reference forward velocity for the robot such that

$$\lim_{t \rightarrow \infty} \|v_t(t) - v_{t,\text{ref}}\| \leq \epsilon_t \quad (22)$$

where $\epsilon_t \in \mathbb{R}_{>0}$ is any arbitrary positive constant. Meanwhile, we aim to keep the normal velocity in a small neighbourhood of the origin such that

$$\lim_{t \rightarrow \infty} \|v_n(t)\| \leq \epsilon_n \quad (23)$$

where $\epsilon_n \in \mathbb{R}_{>0}$ is a constant. Finally, we require that all the solutions of the controlled system remain bounded.

IV. BODY SHAPE CONTROL

In this section, we propose a feedback control law for the body shape of the snake robot. In particular, we stabilize a desired gait pattern for the body shape variables, which induces lateral undulatory forward locomotion on the robot.

It is well-known [4] that the gait pattern lateral undulation for an N -link snake robot will be achieved if every i -th joint of the robot moves in accordance with the reference joint trajectory given by

$$\phi_{\text{ref},i}(t) = \alpha \sin(\omega t + (i-1)\delta) + \phi_o \quad (24)$$

where α denotes the amplitude of the sinusoidal joint motion, ω denotes the frequency of the joint oscillations, and δ denotes a phase shift which is used to keep the joints *out of phase*. Furthermore, ϕ_o is an offset term which can be used for controlling the orientation of the robot in the plane.

In [10], based on analytical investigations using the averaging theory, it was shown that the forward velocity of a snake robot which moves based on the lateral undulatory gait induced by (24), is affected by the gait parameters (α, ω, δ) . Consequently, inspired by the work of [4] and [10], we introduce the following reference for the joint angles of the snake robot,

$$\phi_{\text{ref},i}(\lambda, \phi_o) = \alpha \sin(\lambda + (i-1)\delta) + \phi_o \quad (25)$$

where λ and $\dot{\phi}_o$ are the solutions of two compensators defined below in equations (34) and (42), respectively. In particular, we will use these compensators to control the forward velocity and orientation of the robot, respectively.

A. Virtual Holonomic Constraints

VHC, see e.g. [14-16], are relations of the form $\Phi : \mathcal{Q} \rightarrow \mathbb{R}$ which are called the constraint functions, and they have the property that they can be made invariant by the actions of a feedback controller [15]. In this case we say that the VHC are enforced. In particular, we call them virtual constraints because they do not arise from a physical connection between two variables but rather from the actions of a feedback controller [14]. A similar concept to VHC is artificial constraints. These constraints are defined for velocities and forces, see e.g. [21]. In contrast, however, VHC are defined for position coordinates of the system.

Inspired by the idea of VHC that has effectively been used for motion control of mechanical systems (see e.g. [14-16] for various examples), we consider (25) as a VHC for the body shape variables of the snake robot. Furthermore, these VHC will be enforced through the control input \bar{u} in (19). In particular, (25) is a dynamic VHC in that it depends on the state-evolution of two dynamic compensators.

Associated with constraint functions (25), is the following constraint manifold

$$\Gamma = \{(x, \dot{x}, \phi_o, \dot{\phi}_o, \lambda, \dot{\lambda}) \in \mathbb{R}^{2N+8} : \phi_i = \phi_{\text{ref},i}(\lambda, \phi_o), v_{\phi_i} = \dot{\lambda} \frac{\partial \phi_{\text{ref},i}}{\partial \lambda} + \dot{\phi}_o \frac{\partial \phi_{\text{ref},i}}{\partial \phi_o}\} \quad (26)$$

where $i \in \{1, \dots, N-1\}$. Our control design approach for the snake robot is given in the following two steps:

1. In the first step, we use the control input \bar{u} in (19) to stabilize the constraint manifold (26) for the fully-actuated shape variables of the robot. This induces a forward motion based on the gait pattern lateral undulation for the robot.

2. In the second step, we restrict the dynamics of the system to the invariant constraint manifold (26), where we use λ and $\dot{\phi}_o$ as two additional control terms, which will be used to control the velocity and orientation of the robot, respectively, cf. Fig. 3.

B. Enforcing the VHC for the shape variables of the robot

In order to stabilize the constraint manifold for the shape variables ϕ , we define the following controlled output vector

$$\tilde{\phi} = [\phi_1 - \phi_{\text{ref},1}, \dots, \phi_{N-1} - \phi_{\text{ref},N-1}]^T \in \mathbb{R}^{N-1} \quad (27)$$

The controlled output vector (27) yields a well-defined vector relative degree $\{2, \dots, 2\}$ everywhere on the configuration space. Consequently, we can stabilize the constraint manifold using an input-output linearizing feedback control law [15]. We define this control law as

$$\bar{u} = \ddot{\phi}_{\text{ref}} - K_d \dot{\tilde{\phi}} - K_p \tilde{\phi} \quad (28)$$

where $K_p = \text{diag}\{k_{p_i}\}_{i=1}^{N-1}$ and $K_d = \text{diag}\{k_{d_i}\}_{i=1}^{N-1}$ denote the positive definite diagonal matrices of the joint proportional and derivative controller gains, respectively. By inserting (28) into (19), the error dynamics equation for the

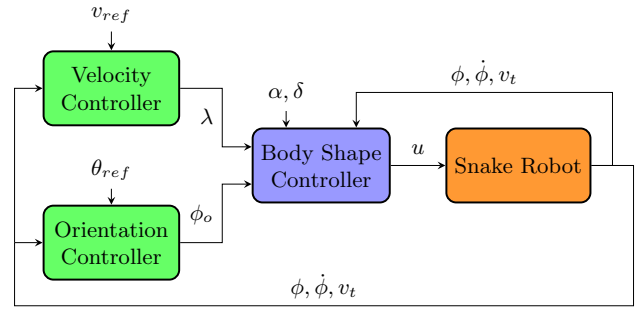


Fig. 3: The Structure of the direction following controller. joint angles of the robot takes the form

$$\ddot{\tilde{\phi}} + K_d \dot{\tilde{\phi}} + K_p \tilde{\phi} = 0 \quad (29)$$

which clearly has a globally exponentially stable equilibrium at the origin $(\tilde{\phi}, \dot{\tilde{\phi}}) = (0_{N-1}, 0_{N-1})$. This implies that joint angle errors converge exponentially to zero, i.e. the constraint manifold is a globally exponentially stable manifold for (10,19), and the control objective (20) will be achieved.

V. ORIENTATION CONTROL

In this section, we control the orientation of the robot by using $\dot{\phi}_o$ as an additional control input on the exponentially stable constraint manifold. To this end, we define the orientation error as

$$\tilde{\theta} = \theta - \theta_{\text{ref}} \quad (30)$$

where $\theta_{\text{ref}} \in \mathbb{R}$ denotes the constant reference orientation of the robot. Furthermore, we derive the orientation error dynamics of the robot evaluated on the constraint manifold. This can be done by writing (11,15) in the error coordinates $(\tilde{\phi}_1, \dots, \tilde{\phi}_{N-1}, \tilde{\theta})$, and then restricting it to the invariant manifold where $(\tilde{\phi}, \dot{\tilde{\phi}}) = (0_{N-1}, 0_{N-1})$. The resulting error dynamics has the form

$$\ddot{\tilde{\theta}} = -\lambda_1 \dot{\tilde{\theta}} + \frac{\lambda_2}{N-1} v_t \bar{e}^T S + \lambda_2 v_t \dot{\phi}_o \quad (31)$$

where $S \in \mathbb{R}^{N-1}$ denotes a vector which is composed of the sinusoidal parts of the reference joint angles (25):

$$S = [\alpha \sin(\lambda), \dots, \alpha \sin(\lambda + (i-1)\delta)]^T \in \mathbb{R}^{N-1} \quad (32)$$

Motivated by the work of [8], where ϕ_o is used as the control input for the orientation dynamics of the snake robot, we use $\dot{\phi}_o$ as a dynamic compensator which controls the orientation of the robot. In particular, we notice that since $\dot{\phi}_o$ is needed for the joint control law (28), then it is more suitable to use this term, i.e. rather than ϕ_o , as the control input to control the orientation. To this end, we take the derivatives of (31) until the control input $\dot{\phi}_o$ appears. The resulting dynamics is of the form

$$\tilde{\theta}^{(4)} = -\lambda_1 \tilde{\theta}^{(3)} + \psi_1(v_t, \phi_o) \ddot{\phi}_o + \psi_2(v_t, v_n, \phi_o, \dot{\phi}_o, \lambda, \dot{\lambda}, \ddot{\lambda}) \quad (33)$$

Note that it is straightforward to derive $\psi_1(\cdot)$ and $\psi_2(\cdot)$ by taking the time-derivatives of (31), however, due to space restrictions, we write them in the symbolic form. We define the input-output linearizing control law

$$\ddot{\phi}_o = \frac{1}{\psi_1} (\lambda_1 \tilde{\theta}^{(3)} - \psi_2 + \sigma) \quad (34)$$

where $\sigma \in \mathbb{R}$ is a new control input which we define as

$$\sigma = -k_3\tilde{\theta}^{(3)} - k_2\tilde{\theta}^{(2)} - k_1\tilde{\theta}^{(1)} - k_0\tilde{\theta} \quad (35)$$

where $k_0, k_1, k_2, k_3 > 0$ denote the orientation controller gains. It can be numerically verified that ψ_1 is bounded away from zero except for very small values of the forward velocity v_t , and this agrees well with the fact that the orientation is not controllable if the forward velocity of the snake robot is zero [10]. We stabilize the origin, i.e. $\tilde{\theta}^{(i)} = 0$ for all $i \in \{0, \dots, 4\}$, of the orientation error dynamics by properly choosing the gains k_i , for instance according to the Routh-Hurwitz stability criterion. Furthermore, we show the boundedness of the solutions of the dynamic compensator (34) through numerical simulations, however, a formal proof of this boundedness remains as a topic of future work. We denote this bound by

$$\|[\phi_o, \dot{\phi}_o]\| \leq \varepsilon \quad (36)$$

where $\varepsilon \in \mathbb{R}_{>0}$. In particular, we denote the upper-bound on each i -th reference joint angle, which is composed of a bounded sinusoidal part and the offset term ϕ_o , as

$$\|\phi_{\text{ref},i}\| \leq \varepsilon^* \quad (37)$$

where $\varepsilon^* \in \mathbb{R}_{>0}$ is a constant.

VI. VELOCITY CONTROL

In this section, inspired by [20], we use the frequency of the joint oscillations as an additional control term to regulate the forward velocity v_t of the robot to a constant reference. Furthermore, we show that the normal velocity v_n of the robot converges to a small neighbourhood of the origin. To this end, we define the velocity errors for the normal and tangential components of the velocity of the CM of the robot as

$$\tilde{v}_t = v_t - v_{t,\text{ref}} \quad (38)$$

$$\tilde{v}_n = v_n - v_{n,\text{ref}} \quad (39)$$

where $v_{t,\text{ref}} \in \mathbb{R}_{>0}$ and $v_{n,\text{ref}} = 0$ denote the reference tangential and normal velocities, respectively. Furthermore, we derive the velocity error dynamics of the robot evaluated on the constraint manifold by writing (16-17) in the error coordinates $(\tilde{\phi}_1, \dots, \tilde{\phi}_{N-1}, \tilde{v}_t, \tilde{v}_n)$, and then restricting them to the invariant manifold where $(\tilde{\phi}, \dot{\tilde{\phi}}) = (0_{N-1}, 0_{N-1})$, which yields

$$\dot{\tilde{v}}_t = -\frac{c_t}{m}(\tilde{v}_t + v_{t,\text{ref}}) + \frac{2c_p}{Nm}\tilde{v}_n\bar{e}^T\Phi_{\text{ref}} + \eta(\dot{\lambda}C + \dot{\phi}_o\bar{e}) \quad (40)$$

$$\dot{\tilde{v}}_n = -\frac{c_n}{m}\tilde{v}_n + \frac{c_p}{Nm}(\tilde{v}_t + v_{t,\text{ref}})\bar{e}^T\Phi_{\text{ref}} \quad (41)$$

where η , C , and Φ_{ref} denote the following vector-valued functions, respectively,

$$C = [\alpha \cos(\lambda), \dots, \alpha \cos(\lambda + (i-1)\delta)]^T \in \mathbb{R}^{N-1}$$

$$\Phi_{\text{ref}} = [\phi_{\text{ref},1}, \dots, \phi_{\text{ref},N-1}]^T \in \mathbb{R}^{N-1}$$

$$\eta = -\frac{c_p}{Nm}\Phi_{\text{ref}}^T A\bar{D} \in \mathbb{R}^{N-1}$$

In the following, we use

$$u_\lambda = \ddot{\lambda} \quad (42)$$

as a control input to regulate the forward velocity of the robot to $v_{\text{ref}} = [v_{t,\text{ref}}, 0]^T \in \mathbb{R}^2$. In particular, we take

$$\dot{\lambda} = \frac{1}{\delta_1} \left(\frac{c_t}{m}v_{t,\text{ref}} - \frac{2c_p}{Nm}\tilde{v}_n\bar{e}^T\Phi_{\text{ref}} - k_\lambda\tilde{v}_t \right) \quad (43)$$

where

$$\delta_1(\phi_o, \lambda) = -\frac{c_p}{Nm}\Phi_{\text{ref}}^T A\bar{D}C = \eta C \quad (44)$$

and where $k_\lambda > 0$ denotes the proportional forward velocity controller gain. It can be numerically verified that $\delta_1(\cdot)$ is uniformly bounded away from zero, and this is because of the phase shift between the link references in (25).

The following theorem investigates the stability of the origin of (40-41).

Theorem I. *a. The origin of the system (40-41) with λ given by the dynamic compensator (42-44) is stabilized provided that $k_\lambda > 0$ is chosen sufficiently high. Furthermore, $\dot{\lambda}$ remains uniformly bounded.*

b. The practical stability of the origin $\tilde{v}_t = 0$ of (40), and convergence of the normal velocity error \tilde{v}_n , which is governed by the dynamical system (41), to a neighbourhood of the origin is achieved with the dynamic compensator (42-44), provided that $k_\lambda > 0$ is chosen sufficiently high. Furthermore, $\dot{\lambda}$ remains uniformly bounded.

Proof of part a: In order to prove the arguments of part a of Theorem I, we iteratively introduce control-Lyapunov functions (CLF) borrowing from the techniques of backstepping (see e.g. [13]), and in addition including a dynamic compensator. In particular, we select the first CLF as

$$V_1 = \frac{1}{2}\tilde{v}_t^2 \quad (45)$$

Taking the time-derivative of (45) along the solutions of (40-41) yields

$$\begin{aligned} \dot{V}_1 &= \tilde{v}_t \dot{\tilde{v}}_t \\ &= \tilde{v}_t \left[-\frac{c_t}{m}v_{t,\text{ref}} - \frac{c_t}{m}\tilde{v}_t + \frac{2c_p}{Nm}\tilde{v}_n\bar{e}^T\Phi_{\text{ref}} + \eta(\dot{\lambda}C + \dot{\phi}_o\bar{e}) \right] \end{aligned} \quad (46)$$

We take $\dot{\lambda}$ defined in (43) as a virtual control input that we use to make (46) negative. For simplicity, we denote

$$\delta_2(\lambda, \phi_o, \tilde{v}_n, \tilde{v}_t) = \frac{1}{\delta_1} \left(\frac{c_t}{m}v_{t,\text{ref}} - \frac{2c_p}{Nm}\tilde{v}_n\bar{e}^T\Phi_{\text{ref}} - k_\lambda\tilde{v}_t \right) \quad (47)$$

For backstepping, we introduce the error variable

$$z = \dot{\lambda} - \delta_2(\lambda, \phi_o, \tilde{v}_n, \tilde{v}_t) \quad (48)$$

which we would like to drive to zero. The dynamic equation of the error variable (48) is given by

$$\dot{z} = u_\lambda - \dot{\delta}_2(\lambda, \lambda, \phi_o, \dot{\phi}_o, \tilde{v}_n, \tilde{v}_t) \quad (49)$$

Note that it is straightforward to derive an analytical expression for $\dot{\delta}_2(\cdot)$, however, because of space restriction we write it in the symbolic form. Furthermore, inserting $\dot{\lambda} = z + \delta_2(\cdot)$ into (46) yields

$$\dot{V}_1 = -k_\lambda\tilde{v}_t^2 - \frac{c_t}{m}\tilde{v}_t^2 + z\tilde{v}_t\delta_1 + \tilde{v}_t\eta\dot{\phi}_o\bar{e} \quad (50)$$

We introduce an augmented CLF of the form

$$V_2 = V_1 + \frac{1}{2}z^2 + \frac{1}{2}\tilde{v}_n^2 \quad (51)$$

Taking the time-derivative of V_2 along the solutions of (40-41) gives

$$\begin{aligned} \dot{V}_2 &= \dot{V}_1 + z\dot{z} + \tilde{v}_n\dot{\tilde{v}}_n \\ &= -k_\lambda\tilde{v}_t^2 - \frac{c_t}{m}\tilde{v}_t^2 + \tilde{v}_t\eta\dot{\phi}_o\bar{e} + z(u_\lambda - \dot{\delta}_2 + \tilde{v}_t\delta_1) + \tilde{v}_n\dot{\tilde{v}}_n \end{aligned} \quad (52)$$

We define the actual control input u_λ in (52) as

$$u_\lambda = \dot{\delta}_2 - \tilde{v}_t\delta_1 - k_z z \quad (53)$$

where $k_z > 0$ is a constant gain. Inserting (53) into (52) yields

$$\dot{V}_2 = -k_\lambda\tilde{v}_t^2 - \frac{c_t}{m}\tilde{v}_t^2 - k_z z^2 + \tilde{v}_t\eta\dot{\phi}_o\bar{e} + \tilde{v}_n\dot{\tilde{v}}_n \quad (54)$$

The last two terms in (54) are indefinite. In particular, $\tilde{v}_n\dot{\tilde{v}}_n$ is of the form

$$\begin{aligned} \tilde{v}_n\dot{\tilde{v}}_n &= \tilde{v}_n \left(-\frac{c_n}{m}\tilde{v}_n + \frac{c_p}{Nm}(\tilde{v}_t + v_{t,\text{ref}})\bar{e}^T \Phi_{\text{ref}} \right) \\ &= -\frac{c_n}{m}\tilde{v}_n^2 + \frac{c_p}{Nm}(\tilde{v}_n\tilde{v}_t + \tilde{v}_n v_{t,\text{ref}})\bar{e}^T \Phi_{\text{ref}} \end{aligned} \quad (55)$$

Using the upper-bound (37), we can write (55) as

$$\tilde{v}_n\dot{\tilde{v}}_n \leq -\frac{c_n}{m}\tilde{v}_n^2 + \frac{2c_p}{Nm}(|\tilde{v}_n||\tilde{v}_t| + |\tilde{v}_n|v_{t,\text{ref}})(N-1)\varepsilon^* \quad (56)$$

In (56), we apply Young's inequality [18] where we have that

$$ab \leq \frac{\gamma a^2}{2} + \frac{b^2}{2\gamma} \quad (57)$$

where $a, b > 0$, and $\gamma \in \mathbb{R}_{>0}$ is any positive constant. Using this inequality, we can write (56) in the form

$$\tilde{v}_n\dot{\tilde{v}}_n \leq -\frac{c_n}{m}\tilde{v}_n^2 + \frac{2c_p}{Nm} \left(\frac{\gamma\tilde{v}_n^2}{2} + \frac{\tilde{v}_t^2}{2\gamma} + \frac{\gamma\tilde{v}_n^2}{2} + \frac{v_{t,\text{ref}}^2}{2\gamma} \right) (N-1)\varepsilon^* \quad (58)$$

Moreover, using the Young's inequality for the term $(\tilde{v}_t\eta\dot{\phi}_o\bar{e})$ we have that

$$\tilde{v}_t\eta\dot{\phi}_o\bar{e} \leq \left| \frac{c_p}{Nm}\bar{e}^T A\bar{D}\bar{e} \right| \varepsilon\varepsilon^* \left(\frac{\tilde{v}_t^2}{2\gamma} + \frac{\gamma}{2} \right) \quad (59)$$

For simplicity we denote

$$\left| \frac{c_p}{Nm}\bar{e}^T A\bar{D}\bar{e} \right| = \zeta \quad (60)$$

Using the inequalities (56-59) in (54), we obtain

$$\begin{aligned} \dot{V}_2 &\leq \left(-k_\lambda - \frac{c_t}{m} + \frac{c_p(N-1)\alpha}{Nm\gamma} + \frac{\zeta}{2\gamma}\varepsilon\varepsilon^* \right) \tilde{v}_t^2 \\ &\quad - k_z z^2 + \left(-\frac{c_n}{m} + \frac{\gamma c_p(N-1)\varepsilon^*}{Nm} \right) \tilde{v}_n^2 + \epsilon \end{aligned} \quad (61)$$

where ϵ denotes the following constant

$$\epsilon = \frac{c_p(N-1)\varepsilon^* v_{t,\text{ref}}^2}{Nm\gamma} + \gamma\zeta\varepsilon\varepsilon^* \quad (62)$$

In order to make the coefficient of \tilde{v}_n^2 negative we need to choose $\gamma < \frac{c_n N}{c_p(N-1)\varepsilon^*}$. For this choice of γ , we can always choose a sufficiently large k_λ such that the coefficient of \tilde{v}_t^2

will be negative as well. In this case we conclude that there exist a sufficiently small positive constant $\beta \in \mathbb{R}_{>0}$ such that the following inequality holds

$$\dot{V}_2 \leq -\beta V_2 + \epsilon \quad (63)$$

Consequently, a straightforward application of the Comparison Lemma (see e.g. [13]) gives

$$V_2(t) \leq V_2(0)e^{-\beta t} + \frac{\epsilon}{\beta} \quad (64)$$

From (64) we conclude that \tilde{v}_n , \tilde{v}_t , and z remain bounded. This implies that the solution exists globally. Moreover, according to (48) $\dot{\lambda}$ remains uniformly bounded, i.e. since z and δ_2 are bounded. Furthermore, V_2 converges to a ball of radius ϵ/β . Because of the quadratic form of (51), $\|\tilde{v}_n\|$ and $\|\tilde{v}_t\|$ converge to a ball of radius

$$r = \sqrt{\epsilon/\beta} \quad (65)$$

Consequently, by properly choosing k_λ , we can drive $\|\tilde{v}_n\|$ and $\|\tilde{v}_t\|$ to a neighbourhood of the origin. This completes the proof of part *a* of Theorem I.

In the following, we will show that it is possible to make $\|\tilde{v}_t\|$ converge to any arbitrary small neighbourhood of the origin, i.e. to be practically stable, and to make $\|\tilde{v}_n\|$ converge to a neighbourhood of the origin. We will show that this can be achieved by choosing k_λ sufficiently large.

Proof of part b: Using the comparison lemma, in (64) we have shown that \tilde{v}_n , \tilde{v}_t , and z are bounded. We denote these bounds by

$$\|\tilde{v}_n\| \leq \delta_{v_n}, \quad \|\tilde{v}_t\| \leq \delta_{v_t}, \quad \|z\| \leq \delta_z \quad (66)$$

where δ_{v_n} , δ_{v_t} , and δ_z are positive scalars. Using these bounds, the time-derivative of V_1 in (50) can be rewritten as

$$\dot{V}_1 \leq -k_\lambda\tilde{v}_t^2 - \frac{c_t}{m}\tilde{v}_t^2 + \delta_z|\tilde{v}_t|\epsilon_1 + |\tilde{v}_t\eta\dot{\phi}_o\bar{e}| \quad (67)$$

where ϵ_1 denotes the upper-bound on δ_1 . Using Young's inequality from (57,59), for (67) we have that

$$\dot{V}_1 \leq -k_\lambda\tilde{v}_t^2 - \frac{c_t}{m}\tilde{v}_t^2 + \frac{(\delta_z\epsilon_1)^2}{2\gamma} + \frac{\gamma\tilde{v}_t^2}{2} + \zeta\varepsilon\varepsilon^* \left(\frac{\tilde{v}_t^2}{2\gamma} + \frac{\gamma}{2} \right) \quad (68)$$

By collecting the coefficients of \tilde{v}_t^2 , (68) can be written as

$$\begin{aligned} \dot{V}_1 &\leq \left(-k_\lambda - \frac{c_t}{m} + \frac{\gamma}{2} + \frac{\zeta\varepsilon\varepsilon^*}{2\gamma} \right) \tilde{v}_t^2 + \frac{(\delta_z\epsilon_1)^2}{2\gamma} + \frac{\gamma\zeta\varepsilon\varepsilon^*}{2} \\ &= -\beta^* V_1 + \frac{(\delta_z\epsilon_1)^2}{2\gamma} + \frac{\gamma\zeta\varepsilon\varepsilon^*}{2} \end{aligned} \quad (69)$$

where

$$\beta^* = 2\left(k_\lambda + \frac{c_t}{m} - \frac{\gamma}{2} - \frac{\zeta\varepsilon\varepsilon^*}{2\gamma} \right) \quad (70)$$

is a constant. Consequently, a straightforward application of the comparison lemma yields

$$V_1 \leq V_1(0)e^{-\beta^* t} + \frac{(\delta_z\epsilon_1)^2}{2\gamma\beta^*} + \frac{\gamma\zeta\varepsilon\varepsilon^*}{2\beta^*} \quad (71)$$

From (71), it can be seen that V_1 converges to a ball of radius $\frac{(\delta_z\epsilon_1)^2}{2\gamma\beta^*} + \frac{\gamma\zeta\varepsilon\varepsilon^*}{2\beta^*}$. Because of (45), $\|\tilde{v}_t\|$ converges to a ball of

radius

$$r_1 = \sqrt{\frac{(\delta_z \epsilon_1)^2}{2\gamma\beta^*} + \frac{\gamma\zeta\epsilon\epsilon^*}{2\beta^*}} \quad (72)$$

Furthermore, we can choose k_λ sufficiently large to drive $\|\tilde{v}_t\|$ to any arbitrary small neighbourhood of the origin, i.e. by making β^* sufficiently large. This completes the proof of part *b* of Theorem I, and the control objectives (22-23) will be achieved.

Remark I. *It is interesting to note from (61) that it is the friction, given by the parameter c_n , that stabilizes the velocity in the normal direction v_n . We have no direct control over v_n , as the snake robot is underactuated, and the oscillations (25) that are induced by the $N - 1$ actuators, create a sideways velocity v_n . Thus, (61) indicates that the friction coefficient c_n needs to be sufficiently large for the system to be stable. This complies with the results concerning controllability of snake robots presented in [19].*

VII. SIMULATION RESULTS

In this section, we present simulation results for the proposed direction following control approach. We considered a snake robot with $N = 10$ links of length $l = 0.14$ m, and mass $m = 1$ kg. The ground friction coefficients were $c_t = 1$ and $c_n = 3$, and the rotation parameters were $\lambda_1 = 0.5$ and $\lambda_2 = 20$. The rotation parameters are chosen such that the simplified model quantitatively behaves similar to the complex model derived in many previous works such as [4,12]. We chose $\alpha = 4.5$ cm, and $\delta = 40\pi/180$. The gains of the exponentially stabilizing joint controller in (28) were set to $k_p = 20$, and $k_d = 5$. The orientation controller gain in (33) were tuned as $k_0 = 5$, $k_1 = 26$, $k_2 = 39$, and $k_3 = 20$. The velocity controller gains were tuned as $k_\lambda = 20$ and $k_z = 0.5$. The tangential reference velocity was $v_{t,\text{ref}} = 0.2$ m/s, and the orientation reference angle was $\theta_{\text{ref}} = \pi/4$. Since on the constraint manifold, where a lateral undulatory gait is stabilized, v_t is positive [10], the initial tangential velocity was chosen as $v_t(0) = 0.1$ m/s, see the arguments after (35), yet all other states are set initially to zero.

The results of the simulations are shown in Fig. 4-10. In Fig. 4 the solutions $\dot{\lambda}$ and ϕ_o of the dynamic compensators are shown. In particular, the frequency of the joint oscillations converges to a positive constant, which according to the work of [4] implies a forward motion for the robot, and ϕ_o remain uniformly bounded. Fig. 5 illustrates the motion of the snake robot in the $x - y$ plane, and how the snake robot follows a path heading in the direction given by the reference. Fig. 6 shows the forward velocity v_t converges to the constant reference velocity $v_{t,\text{ref}}$. Fig. 7 shows that the normal velocity converges to a small neighbourhood of the origin. In Fig. 8 it can be seen that the body shape variables follow the reference joint angles (25), while the norm of the error converges exponentially to zero. Fig. 9 shows that the proposed orientation controller (34) successfully reorients the robot in accordance with θ_{ref} . Finally, Fig. 10 shows that the coefficients of the virtual control inputs in (34,43) are globally well-defined.

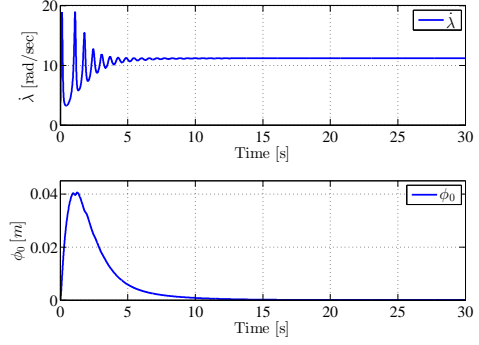


Fig. 4: The solutions of the dynamic compensators remain bounded.

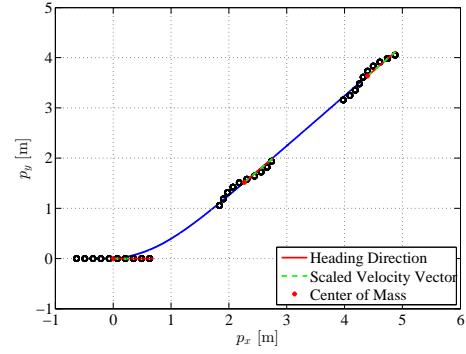


Fig. 5: A 10-links snake robot follows the desired orientation.

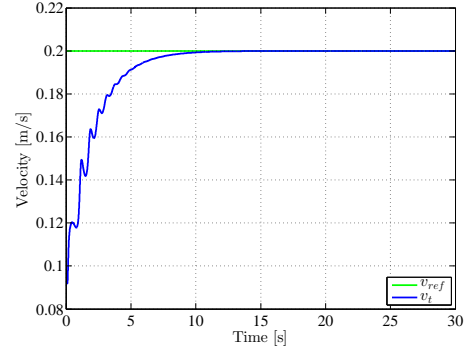


Fig. 6: The forward velocity of the robot is regulated to the constant reference velocity.

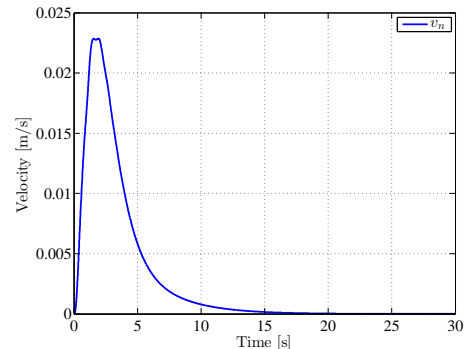


Fig. 7: The normal velocity of the robot converges to a small neighbourhood of the origin.

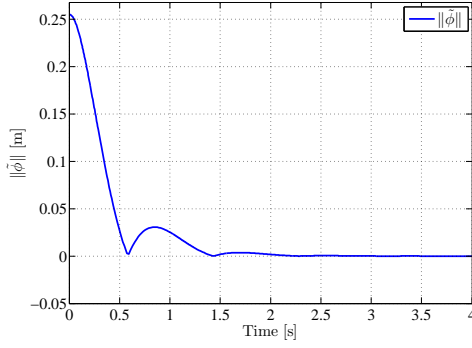


Fig. 8: The joints angles converge to the reference joint angles.

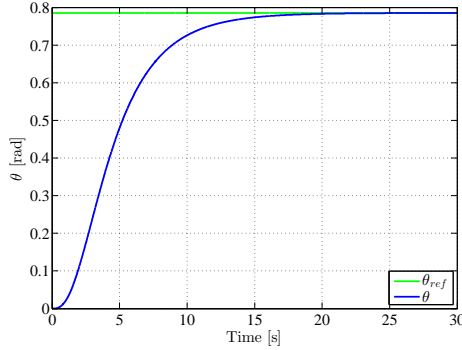


Fig. 9: The orientation of the robot converges to the reference orientation.

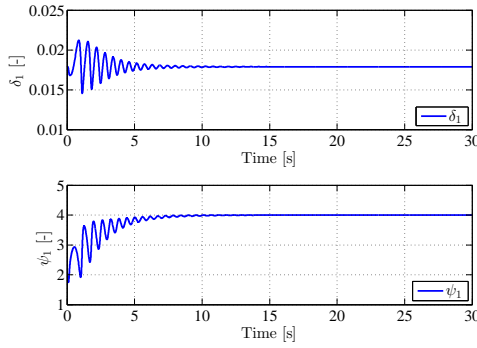


Fig. 10: The coefficients of the control inputs in (34,43) are globally well-defined.

VIII. CONCLUSION

We considered direction following control of planar snake robots using the method of virtual holonomic constraints, based on a simplified dynamic model developed for control design and analysis purposes in [10]. We enforced virtual holonomic constraints for the body shape variables of the robot. These constraints were inspired by the well-known reference joint angle trajectories which induce lateral undulatory gait pattern on snake robots. Furthermore, we removed the explicit time-dependence of the reference joint angles, and rather, made them a function of the solutions of two dynamic compensators. Subsequently, we reduced the dynamics of the system to the invariant constraint manifold, where we used the dynamic compensators to control the velocity and orientation of the robot. Simulations results were presented which showed the performance of the theoretical approach.

REFERENCES

- [1] S. Tully, G. Kantor, M.A. Zenati, and H. Choset, "Shape Estimation for Image-Guided Surgery with a Highly Articulated Snake Robot", in Proc. 2011 IEEE/RSJ Int. Conf. on Intelligent Robots and Systems, San Francisco, CA, USA, Sep. 2011.
- [2] P. Chatzakos, Y.P. Markopoulos, K. Hrissagis, and A. Khalid, "On the development of a modular external-pipe crawling omni-directional mobile robot", *Industrial Robot: An International Journal*, Vol. 33, no. 4, pp. 291-297, 2006.
- [3] Z. Wang, E. Appleton, "The concept and research of a pipe crawling rescue robot.", *Advanced Robotics*, vol.17, no.4, pp: 339-358, 2003.
- [4] S. Hirose, "Biologically Inspired Robots: Snake-Like Locomotors and Manipulators", Oxford University Press, 1993.
- [5] P. Prautsch, T. Mita, and T. Iwasaki, "Analysis and control of a gait of snake robot", Transactions-Institute of Electrical Engineers of Japan, D-120.3. pp. 372-381. 2000.
- [6] H. Date, Y. Hoshi, and M. Sampei, "Locomotion control of a snakelike robot based on dynamic manipulability", in Proc. the IEEE/RSJ Int. Conf. on Intelligent Robots and Systems, Takamatsu, Japan, 2000.
- [7] S. Ma, Y. Ohmameuda, K. Inoue, and B. Li, "Control of a 3-dimensional snake-like robot", in Proc. IEEE Int. Conf. Robotics and Automation, vol. 2, pp.2067-2072, Taipei, Taiwan, 2003.
- [8] M. Tanaka and F. Matsuno, "Control of 3-dimensional snake robots by using redundancy", in Proc. IEEE Int. Conf. Robotics and Automation, pp.1156-1161, Pasadena, CA, 2008.
- [9] G. Hicks and K. Ito, "A method for determination of optimal gaits with application to a snake-like serial-link structure", *IEEE Transactions on Automatic Control*, vol. 50, no. 9, pp.1291-1306, 2005.
- [10] P. Liljebäck, K.Y. Pettersen, Ø. Stavdahl, and J.T. Gravdahl, "Snake Robots - Modelling, Mechatronics, and Control", Advances in Industrial Control, Springer, 2013.
- [11] P. Liljebäck, I.U. Haugstuen, and K.Y. Pettersen, "Path following control of planar snake robots using a cascaded approach", *IEEE Transactions on Control Systems Tech.*, vol. 20, 111-126, 2012.
- [12] E. Rezapour, K.Y. Pettersen, P. Liljebäck, J.T. Gravdahl and E. Kelasidi, "Path Following Control of Planar Snake Robots Using Virtual Holonomic Constraints: Theory and Experiments", *SpringerOpen Journal of Robotics and Biomimetics*, 2014.
- [13] H.K. Khalil, "Nonlinear Systems", Third ed., Englewood cliffs, NJ: Prentice-Hall, 2002.
- [14] E.R. Westervelt, J.W. Grizzle, C. Chevallereau, J. H. Choi, and B. Morris, "Feedback control of dynamic bipedal robot locomotion", Boca Raton: CRC press, 2007.
- [15] M. Maggiore, and L. Consolini, "Virtual Holonomic Constraints for Euler-Lagrange Systems," *IEEE Transactions on Automatic Control*, vol.58, no.4, pp.1001-1008, 2013.
- [16] A. Shiriaev, J.W. Perram, and C. Canudas-de-Wit, "Constructive tool for orbital stabilization of underactuated nonlinear systems: Virtual constraints approach", *IEEE Transactions on Automatic Control*, 50.8: 1164-1176, 2005.
- [17] X. Yang, "Practical stability in dynamical systems", *Chaos, Solitons Fractals*, vol.11 no.7, pp-1087-1092, 2000.
- [18] V.I. Arnol'd, "Mathematical methods of classical mechanics", Vol. 60. Springer, 1989.
- [19] P. Liljebäck, K.Y. Pettersen, O. Stavdahl, and J. T. Gravdahl, "Controllability and stability analysis of planar snake robot locomotion", *IEEE Transactions on Automatic Control*, vol. 56(6):1365-1380, 2011.
- [20] A. Mohammadi, E. Rezapour, M. Maggiore, and K.Y. Pettersen, "Direction Following Control of Planar Snake Robots Using Virtual Holonomic Constraints", 53rd IEEE Conf. on Decision and Control, Los Angeles, CA, USA, Dec 2014.
- [21] M.W. Spong, S. Hutchinson, and M. Vidyasagar, "Robot modeling and control", New York: John Wiley and Sons, 2006.